ELSEVIER

Physica B 217 (1996) 181–192

PHYSICA B

Investigation of the transport properties of gold point contacts

L. Weber, M. Lehr, E. Gmelin*

Max-Planck-Institut für Festkörperforschung, Heisenbergstraße 1, Postfach 800660, D-70506 Stuttgart, Germany

Received 15 August 1995; in final form 11 September 1995

Abstract

Electrical resistance, thermal resistance and thermoelectric power of gold point contacts with well-defined surface properties are investigated in the temperature range 2–300 K. The electrical contact resistance is temperature independent, the thermopower strongly decreases with reduction of the contact size, and an asymmetric heat release, expected for ballistic charge transport, is not detected. We conclude that electronic transport in microcontacts made of gold is strongly afflicted by surface layers. Even a monoatomic layer of impurity atoms creates a tunneling barrier that prevents ballistic carrier transport. Earlier experiments on the transport properties of mechanical point contacts are critically reviewed and discussed with respect to the present results.

1. Introduction

Ballistic charge transport, that is the movement of charge carriers without scattering, is an interesting topic of solid state physics. The precondition for the occurrence of ballistic transport is that the mean free path of the charge carriers l is much larger than the geometrical size of the sample. In the case of point contacts the relevant size is given by the contact radius a. To fulfil the condition $l \gg a$ small contacts and low temperature are required. Mechanical point contacts are of particular advantage for the observation of ballistic phenomena since electrons *and* phonons are simultaneously submitted to the same geometrical restrictions.

Ballistic transport of charge carriers has important applications not only in solid state research (for instance, the investigation of the electron–phonon interaction by point contact spectroscopy), but it is of increasing interest in the field of microelectronics [1, 2]. Whereas the electrical effects, caused by ballistic transport, are object of intensive scientific research, the thermal and thermoelectric effects are only scarcely investigated [3–14]. In the present work we focus on the transport properties of *mechanical point contacts*. In particular, we investigate the so-called heat asymmetry, that is the asymmetric production of Joule's heat in ballistic point contacts with respect to the contact plane. The physical background of this effect is not yet fully understood. The existing results of experimental and theoretical investigations are vague and inconsistent [15–20]. Accurate and reliable measurements of the heat asymmetry on well-defined samples are still missing.

In the present work we present new experiments of Joule's heat release in homogeneous gold point contacts. The measurements are performed using an improved measuring device, that provides optimum experimental conditions for the observation of the heat asymmetry. In Section 2 we shortly explain the physical origin of the heat asymmetry. Section 3 contains a survey of the experimental

* Corresponding author.

SSDI 0921-4526(95)00630-3

setup and the measuring method used and informs about the sample preparation and the properties of the sample material. The experimental results (electrical and thermal contact resistance, current–voltage characteristic, thermoelectric power, and heat asymmetry) are presented and discussed in Section 4. Section 5 finally summarizes the present work.

2. Origin of the heat asymmetry

In the following section we discuss the physical origin of the heat asymmetry in point contacts. Instead of presenting a detailed theoretical analysis, we confine ourselves to a simple classical treatment in order to illustrate how ballistic charge transport gives rise to an asymmetric production of Joule's heat. The upper part of Fig. 1 schematically shows the usual point contact model, namely a circular orifice in an electrical and thermal isolating plane. The application of a bias voltage V_0 causes the electrons to move from the negative to the positive side of the contact. On condition that the mean free path of the charge carriers l is much larger than the contact radius a, the electrons pass the contact ballistically, i.e. without scattering events. Scattering mainly takes place outside of the contact area, in a distance which is much larger than the contact radius. According to the lower part of Fig. 1 the electrical field strength E inside of the sample diverges from zero only in a very small area around the point contact. The voltage and the electrical field strength along the longitudinal axis of the contact are given by

$$V = \frac{V_0}{2} \frac{z}{\sqrt{z^2 + a^2}}, \tag{1}$$

$$E = -\frac{\mathrm{d}V}{\mathrm{d}z} = -\frac{V_0}{2a} \frac{1}{\sqrt[3]{1 + (z/a)^2}}, \tag{2}$$

where z is the distance from the contact plane [21, 22]. Passing through the point contact the electrons are accelerated in the electrical field and gain an additional kinetic energy eV_0. The electrons have no possibility for energy relaxation in-

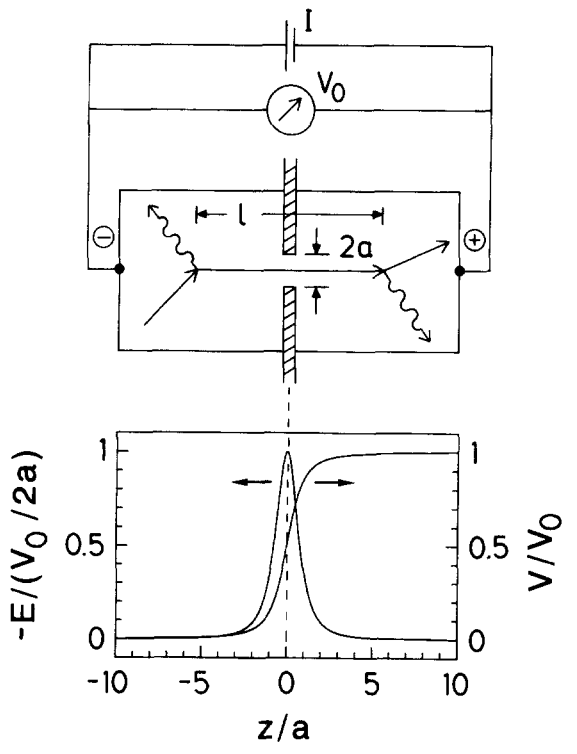

Fig. 1. Upper part: Schematic model of a ballistic point contact. The mean free path of the electrons l is much larger than the contact radius a. Lower part: Voltage V and electrical field strength $E = -\mathrm{d}V/\mathrm{d}z$ along the longitudinal axis of the point contact. At a distance of $z = 5a$ from the contact plane the field strength has decreased to less than 1% of its maximum value $E_{\max} = V_0/2a$.

side of the contact area because of their ballistic motion. Instead, the kinetic energy is released by Joule's heat production in the bulk material far away from the contact. The heating power $\dot{Q} = IV_0$ (I is the electrical current) is mainly released on the downstream side (positive side) of the point contact, so that a temperature gradient across the contact arises. This effect is called heat asymmetry. Theoretically, the relative asymmetry $(\dot{Q}_+ - \dot{Q}_-)/(\dot{Q}_+ + \dot{Q}_-)$ (the indices + and − refer to the positive and the negative sides of the contact, respectively) can reach almost 100%. In practice, however, this value is reduced by a backflow of heat across the point contact and by production of Joule's heat in the sample material and the electrical leads.

According to detailed theoretical investigations of the heat asymmetry in metallic and semiconducting point contacts, the relative asymmetry mainly consists of two contributions: the electronic component A_e, which is due to the acceleration of the electrons in the electrical field, and the phononic part A_p, corresponding to the anisotropic generation of phonons by nonequilibrium electrons [15, 16]. For metallic point contacts the electronic component can be estimated by

$$A_e \sim \frac{eV_0}{\varepsilon_F}. \tag{3}$$

Inserting $V_0 = 10$ mV (a typical measuring voltage) and $\varepsilon_F = 5.5$ eV (the Fermi energy of gold) into Eq. (3) yields $A_e \simeq 0.002$. Because of the small numerical value of A_e the heat asymmetry of gold point contacts is mainly determined by the phononic contribution A_p. For $eV_0 \gtrsim k_B\Theta_D$ the phononic component can be expressed as

$$A_p \sim \frac{2ak_B^2\Theta_D^2}{eV_0\hbar v_F}, \tag{4}$$

where $\Theta_D \simeq 180$ K and $v_F = 1.4 \times 10^6$ m/s are the Debye temperature and the Fermi velocity of gold, respectively.

3. Experimental setup

Since a detailed description of the experimental setup has already been published [23], we restrict to a short introduction into construction and operation of the measuring device. A more detailed description is reserved for those components of the setup that are especially designed for detection of the heat asymmetry.

3.1. Survey of the experimental setup

The point contacts are produced by pressing two sharp-edged gold wedges, crosswise against each other, such as shown in Fig. 2. (The basal plane of the wedges has an area of about 3.5×6 mm^2. The cross-section is a rectangular triangle.) The contact size can be varied continuously by adjusting the mechanical force between the wedges. One of the samples is coupled to a temperature-controlled heat sink. The other one is thermally isolated and equipped with a small heater. By heating of the isolated sample we can create a temperature difference between the wedges, which is measured by a low-temperature thermocouple (0.07 at% Fe in Au versus chromel) and a nano-voltmeter. The absolute temperature is determined by calibrated germanium and platinum resistance thermometers.

For determination of the thermal resistance of the point contact $W_{pc} = \Delta T/J$ (ΔT is the temperature difference between the wedges and J the heat flow across the contact), we apply a constant heating power to the thermally isolated wedge and measure the resulting temperature difference by means of the thermocouple. In order to achieve accurate measuring results, the temperature difference is adjusted between 1% (at $T = 300$ K) and at most 10% (at $T = 4.2$ K) of the absolute temperature. Since the heat flow across the contact is very small, residual heat losses by electrical leads, mechanical support, and thermal radiation have to be considered carefully. This is realized by performing two independent measurements of the thermal resistance: the residual resistance W_{res} and the total resistance W_{tot} are measured with the contact open and closed, respectively. Since W_{res} and W_{pc} are arranged in parallel, the thermal resistance of the

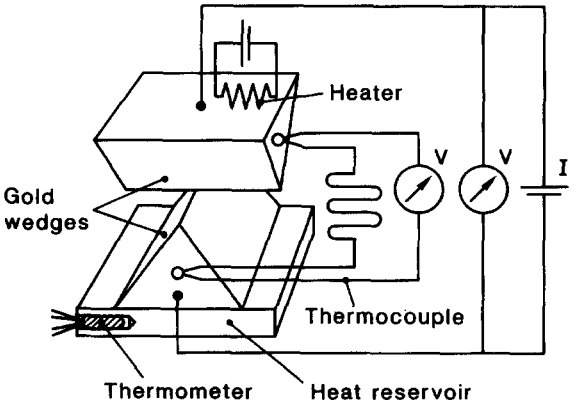

Fig. 2. Schematic diagram of the experimental setup.

point contact can be calculated by

$$W_{pc} = \frac{W_{res} \times W_{tot}}{W_{res} - W_{tot}}. \quad (5)$$

With the outlined experimental arrangement electrical resistance, thermal resistance, and thermoelectric power of the point contact can be measured simultaneously. The measurements are performed in two experimental devices. The low-temperature device enables measurements in the temperature range 1.5–300 K and application of magnetic fields up to 5 T. In an ultra-high vacuum device we can clean the samples by Argon sputtering and analyze the composition of the sample surface by Auger electron spectroscopy.

To measure the heat asymmetry, the required heating power is produced by an electrical current flowing through the point contact. If ballistic charge carrier transport occurs, the heat is mainly released in that wedge, which is connected to the positive terminal of the current source. If the thermally isolated sample is positively charged the production of Joule's heat causes the emergence of a temperature difference between the wedges. At reverse polarity, however, the heat flows off into the heat reservoir, so that the resulting temperature difference is almost zero. The relative asymmetry of heat release $\alpha = (\dot{Q}_+ - \dot{Q}_-)/(\dot{Q}_+ + \dot{Q}_-)$ can thus be determined by measuring the temperature difference ΔT between the wedges depending on magnitude and polarity of the electrical current. Carrying out the measurement by using a constant current, the relative heat asymmetry is given by the measured temperature difference:

$$\alpha = \frac{\Delta T_p - \Delta T_n}{\Delta T_p + \Delta T_n}, \quad (6)$$

where the indices p and n represent the positive (p) and negative (n) direction of the current, respectively.

3.2. Details of the experiment

To determine the heat asymmetry we must perform very precise measurements of Joule's heat production. Such measurements require a large thermal resistance between the thermally isolated wedge and the heat reservoir ($W_{res} \simeq 4 \times 10^4$ K/W at liquid helium temperature) and an accurate measurement of the temperature difference between the wedges (resolution better than 1 mK in the whole temperature range). According to the above-mentioned specifications of the measuring device the heating power is determined with a resolution of 3×10^{-8} W, that is less than 0.1% of the Joule's heat to be measured.

The thermal insulation of the upper sample could be easily improved by using longer and thinner lead wires, since at low temperatures heat transfer mainly takes place by thermal conduction within the electrical leads. On the other hand, lengthening of the leads would enlarge the production of Joule's heat, which would result in a reduction of the measuring effect, since the generated heat partly flows off into the samples. The present lead dimensions are a compromise: The leads consist of gold wires with a length of 32 cm, a diameter of 78 μm, and an electrical resistance of about 7×10^{-3} Ω at liquid helium temperature. Because of the strong thermal insulation the mass of the isolated sample holder must be small enough to achieve useful relaxation times of the experimental setup. We reach relaxation times of about 20 min at room temperature and 1 min at liquid helium temperature using a sample holder with a mass of 450 mg (including the mass of the gold sample of about 350 mg).

To estimate the number of ballistic charge carriers we need trustworthy data of the radius of the point contact. Since, as is shown in Section 4, the electrical and thermal transport properties of gold contacts are strongly affected by surface layers, the usual methods for determination of the contact size by use of the electrical and thermal contact resistance (as described in Ref. [23]) are likewise not applicable. Instead, the contact radius is estimated by measuring the contact force considering the geometrical form of the sample wedges [23, 24]. (An exact determination of the contact size is not always possible by this way since the mechanical pressure in the center of the contact partly reaches the elastic limit of the sample material, so that the sample edge may be durably deformed.) For the investigated gold samples such effects have been avoided; the useful range of force is 10^{-5}–10^{-2} N corresponding to a contact radius of about 0.5–5 μm.

The contact force is generated by attaching one of the samples to 3 small springs with a total resilience of about 14 N/m. (The springs consist of tungsten wire with a diameter of 92 μm. Each spring has a length of 5.5 mm, a diameter of 3.5 mm, and contains 8 free turns.) The second sample can be displaced in such a manner that the springs are compressed and the contact force is modified. The displacement is carried out by a mechanical gear (driven by a stepping motor) in combination with a piezoelectric actuator (resolution about 5 nm) [23]. Because of the small resilience of the springs and the high resolution of the actuator the contact force can be adjusted almost continuously. The thermal expansion of the measuring cell is generally much smaller than the compression of the springs, so that the variation of the temperature does not effect the contact size.

3.3. Sample preparation

The investigated samples consist of gold with a purity of 99.995%. Since even very small traces of ferromagnetic impurities cause large variations of the thermoelectric power of gold at low temperatures [25, 26], the wedges and the lead wires are made from the same batch of sample material. The production of the samples is carried out by cutting the gold wedges and grinding their surfaces. The wires are produced by pulling the raw material through sapphire nozzles with gradually decreasing diameter. The samples are submitted to an ultrasound cleaning in acetone and distilled water after the mechanical treatment, and then annealed at about 1100 K in an inert atmosphere for several hours to remove crystalline defects.

The electrical contacts between the wedges and the electrical leads are made by strongly pressing the ends of the lead wires against the lateral surfaces of the wedges. The samples are again heated to a temperature of 1100 K after fabrication of the mechanical connections, so that wedges and wires weld together. The generation of Peltier heat at the electrical contacts, which can lead to systematic errors in determination of the heat asymmetry, is savely prevented by use of the described experimental arrangement. Since the whole electrical circuit consists of the same material, the measured thermoelectric voltage directly represents the change of the bulk thermopower at the point contact.

3.4. Properties of the sample material

For characterization of the sample material, we investigate the electrical conductivity σ as a function of temperature. The results of our measurements ($\sigma = 4.3 \times 10^5\ \Omega^{-1}\,\mathrm{cm}^{-1}$ at room temperature and $\sigma = 9.1 \times 10^7\ \Omega^{-1}\,\mathrm{cm}^{-1}$ at liquid helium temperature) are in good agreement with previous investigations on comparable samples [27]. According to literature the thermal conductivity κ and the thermoelectric power S of gold at room temperature amount to about $\kappa = 3.0$ W/(cm K) and $S = +1.9$ μV/K, respectively [28, 29]. (At low temperatures universally valid data are not available, since the thermal and thermoelectrical properties of gold in this temperature range strongly depend on the type and the concentration of the included impurity atoms.) The conduction of heat in gold almost completely takes place by electrons, remaining valid even at low temperatures [30].

The mean free path of the electrons l_e is estimated from the measured electrical conductivity by means of the kinetic transport theory:

$$l_e = \frac{\sigma m_e v_F}{ne^2}, \tag{7}$$

where m_e is the electronic mass, v_F is the Fermi velocity, and n is the density of the conduction electrons. The application of the above equation provides a mean free path of the electrons of about $l_e = 0.04$ μm at room temperature and $l_e = 7.5$ μm at liquid helium temperature. Since the radius of the investigated point contacts can be adjusted in the range of about 0.5–5 μm (as estimated from the contact force and the sample geometry), the experimental conditions which are necessary for observation of ballistic charge transport at low temperatures are in principle fulfilled.

4. Experimental results

The following section describes the results of our measurements on gold point contacts. We critically

discuss the experimental data in consideration of perturbing effects and shortly review previous experimental and theoretical investigations.

4.1. Electrical and thermal conduction

The electrical and thermal properties of mechanical point contacts strongly depend on the purity and microstructure of the contact surface. Even at contacts which consist of noble metals such as gold and platinum, the surface of the contact members is covered by insulating layers, either due to oxidation or to the adsorption of gas molecules [7–9]. The existence of surface layers can only be avoided by special experimental precautions, such as, for instance, by ultra-high vacuum.

The high mechanical stress arising in the center of mechanical point contacts may lead to local damage of the surface layer, so that the electrons can pass the contact through small conducting inclusions inside of the barrier. However, even if the barrier is damaged, the metallic charge transport is superimposed by the tunneling of electrons through the intact parts of the barrier. Thus, the dominating transport mechanism is determined by the magnitude of the mechanical stress as well as by chemical structure and the thickness of the insulating layer.

The understanding of the observed thermal and thermoelectrical phenomena essentially depends on whether the electrical transport mainly occurs by tunneling or by metallic conduction. Informations about the dominating transport mechanism result from comparison of the electrical and thermal contact resistance. Since the heat transport in gold – even at low temperatures – almost exclusively takes place by electrons, electrical and thermal contact resistance are connected by the Wiedemann–Franz law:

$$W = \frac{R}{TL}, \tag{8}$$

where $L = (\pi^2/3)(k_B/e)^2$ denotes the Lorenz number. This relation, that applies to clean contacts, remains valid in the presence of thin tunneling barriers [31]. In thick barriers, however, which are almost impervious for electrons, the heat transport by phonons is no longer negligible, so that the thermal resistance falls below the value predicted by the Wiedemann–Franz law (the phononic heat conduction is much less impeded by surface layers than the electronic contribution).

An example for this effect is shown in Fig. 3, where electrical and thermal contact resistance are compared with each other. Before cleaning of the samples, the thermal resistance lies considerably (by approximately a factor of 3) below the solid line representing the Wiedemann–Franz law. The deviations almost disappear after removal of the surface layer by etching. (The etching is carried out by means of aqua regia, which is a mixture of concentrated hydrochloric acid, HCl, and nictric acid, HNO_3, in the ratio 1:3. The etching time is about 20 s. After etching the samples are cleaned in distilled water, dried by an acetone dip and immediately placed into the measuring cell, so that they are exposed to air for less than 1 h.) All further measurements presented in this paper are carried out using etched samples.

To examine, whether the etching process is sufficient to prevent completely tunneling, we investigate the temperature dependence of the contact resistance at fixed contact size. Measurements like that are a sensitive method for determination of the transport mechanisms because the tunneling resistance is almost temperature independent [32],

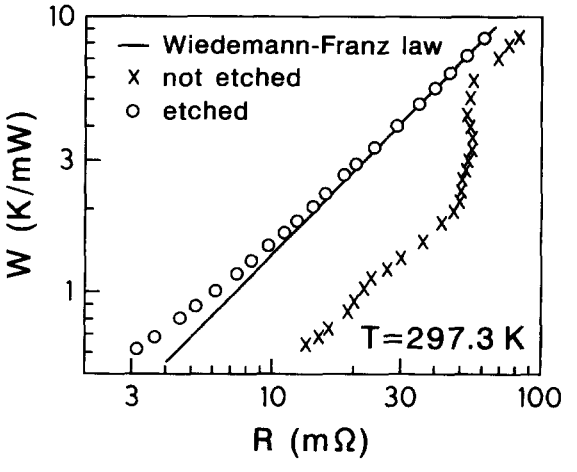

Fig. 3. Relation between electrical and thermal contact resistance, R and W, before and after etching of the samples. The solid line represents the Wiedemann–Franz law $W = R/(TL)$.

whereas the ohmic contact resistance – above the range of residual resistivity – strongly varies with temperature. The temperature dependence of the contact resistance and of the electrical resistivity should coincide for clean contacts. For such clean contacts, without tunneling barrier, the contact resistance is given by the following expression which applies for diffusive charge transport ($l \ll a$):

$$R = \frac{\rho}{2a}, \tag{9}$$

where $\rho = 1/\sigma$ is the electrical resistivity of the sample material.

In our experiments on gold point contacts, however, we generally observe a *temperature-independent* behavior of the contact resistance. A typical measurement at temperature between 2 and 50 K is displayed in Fig. 4. The contact resistance remains constant within 2%, whereas the electrical resistivity varies by a factor of 20.

We note that in the case of ballistic charge transport the contact resistance behaves likewise temperature-independent. For that reason we create measuring conditions (large contacts and high temperatures) which prevent ballistic transport. Since all measurements yield similar results, we conclude that the charge transport in gold point contacts – in spite of etching – mainly takes place by tunneling.

As a further attempt to remove the tunneling barrier, we place the samples into an ultrahigh-vacuum chamber ($p < 10^{-9}$ mbar) and clean the surface by sputtering with 5 keV argon ions. Also this treatment does not substantially change the electrical properties in comparison with etching. The remaining tunneling barrier may be due to the adsorption of gas molecules from the residual gas (an Auger spectrum of the sample surface is shown in Fig. 5) or more probably to the generation of defects and dislocations at the sample surface by sputtering.

4.2. Current–voltage characteristic

The investigation of the current–voltage characteristics of point contacts provides information about the electron–phonon interaction and the phonon density of states in solids. The electrons are

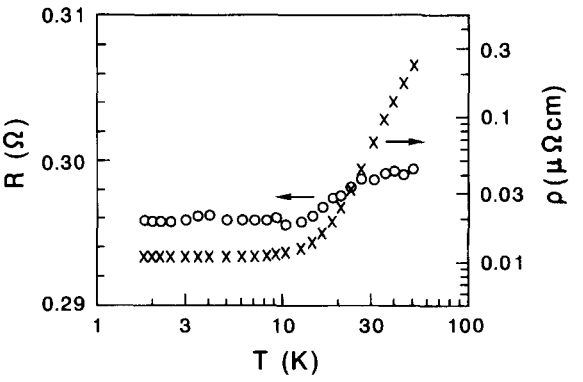

Fig. 4. Temperature dependence of the contact resistance R (at fixed contact size) and the electrical resistivity of the sample material ρ. (Note the different scaling of the left and right ordinate axis.)

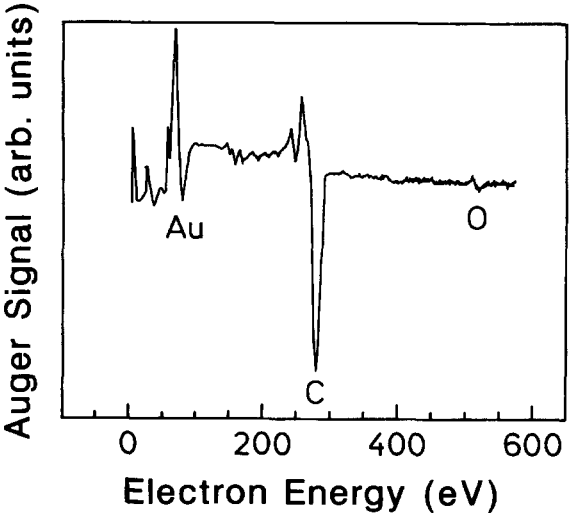

Fig. 5. Auger spectrum of the surface of the gold samples shortly after sputtering. The oxygen and carbon peaks are due to the adsorption of gas molecules from the residual gas.

strongly accelerated by the electrical field in the contact area. After they have passed through the contact, they release their energy by inelastic collisions with phonons. A small number of electrons is scattered back to the contact they came from, so that the electrical current through the contact is reduced causing a non-linear shape of the current–voltage characteristic. As is shown by theoretical calculations, the second derivative of the current–voltage characteristic d^2I/dV^2 is proportional

to the Eliashberg function $\alpha^2(\omega)F(\omega)$, where $\alpha^2(\omega)$ and $F(\omega)$ are the squared matrix element of the electron–phonon interaction and the phonon density of states, respectively [21].

Point contact spectroscopy, i.e. the measurement of the second derivative of the current–voltage characteristics of microcontacts, have been performed with various materials such as metals, metallic alloys and superconductors [33]. Ballistic movement of the electrons through the contact is not necessarily required for point contact spectroscopy. This measuring method is also possible (with decreased sensitivity) if the charge transport takes place by diffusion on condition that the relation $d < (l_e l_i)^{1/2}$ is valid, where d is the contact diameter and l_e and l_i are the elastic and inelastic electron scattering lengths, respectively [34, 35].

In this work the second derivative of the current–voltage characteristic d^2I/dV^2 is determined by modulation of the measuring current by a small AC current of usually less than 1% of the DC component. The resulting AC voltage is measured by phase-sensitive detection at twice the fundamental frequency to obtain a signal which is proportional to d^2I/dV^2. A typical measuring curve, recorded at a temperature of 3.8 K, is shown in Fig. 6. The shape of the curve corresponds quite well with the solid line, that represents the phonon density of states obtained from neutron scattering experiments [36]. A comparison of the two curves reveals that the electrons are less strongly coupled to the longitudinal (high-energy) phonons than to the transverse phonons. The results obtained are in good agreement with previous investigations on gold point contacts [37].

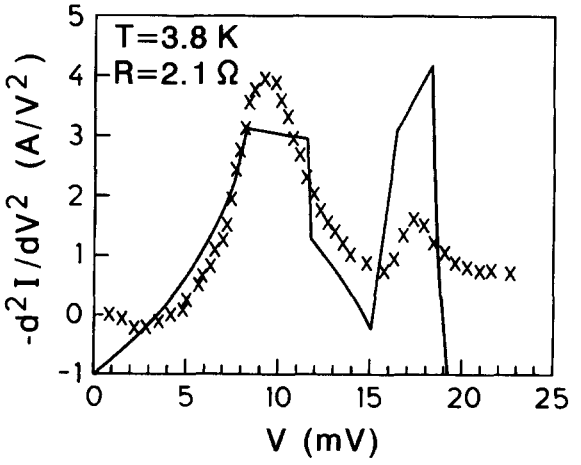

Fig. 6. Second derivative of the current–voltage characteristic as a function of the applied voltage. The solid line represents the phonon density of states according to the literature.

The physical properties of the investigated point contacts noticeably depend on the position of the contacts at the sample surface. This is a result of surface contamination. The shown results are typical examples of the measured data. The properties of most contacts are quite similar. Some few contacts, however, display a different behavior as, for example, the missing of visible structures in the current–voltage characteristic.

4.3. Thermoelectric power

Investigations of the thermopower of mechanical point contacts have been performed on several materials such as noble metals (copper, silver, gold and platinum) and semiconductors (silicon, germanium and gallium arsenide with different types and concentration of impurity atoms) [7–10, 12, 14]. All point contact experiments give qualitatively similar results, namely, a distinct decrease of the thermopower that takes place with the reduction of the contact size.

In the experimental arrangement used, the contact members and the electrical leads consists of the same material. Usually, no thermoelectric voltage can be observed in a homogeneous chain like that under non-ballistic conditions. However, if the thermoelectric properties of the point contact are changed (for instance, by reduction of the contact size) the chain loses its homogeneity, so that the application of a temperature gradient across the contact ΔT generates a thermoelectric voltage V [20, 31]. The measuring signal $S = V/\Delta T$ therefore represents the difference between the bulk value S_b and the point contact value S_{pc} of the thermopower. An increase of the measuring signal thus corresponds to a reduction of the thermopower in the contact region.

At gold point contacts the reduction of the thermopower typically amounts to about 50% of the original value in the bulk material. The physical reasons of this effect are not yet fully understood. In

the following, we shortly review the existing theories and discuss whether they apply to our measuring results.

The large temperature gradient in the center of mechanical point contacts gives rise to the formation of a *non-equilibrium carrier distribution*, which can considerably reduce the thermopower in the contact region (Benedicks effect) [38–40]. To investigate the eventual occurrence of the Benedicks effect in gold point contacts, we vary the temperature difference between the contact sides ΔT and measure the resulting change of the thermopower. The measurement is carried out with fixed contact size at a mean temperature of about 297 K. In the measuring range of $\Delta T = 0.2 - 20$ K the thermopower changes by less than 2%, so that the influence of the Benedicks effect is found to be negligibly small.

The *mechanical stress* in the center of point contacts can reach very high values, which often exceed the limit of elastic deformation. The high-pressure leads to distortion of the crystal lattice and the band structure and generates additional scattering centers in the contact area. In semiconducting point contacts the mechanical pressure has shown to be the main reason for the dependence of the thermopower on the contact size [14]. In metals, however, the physical consequences of mechanical stress are much less pronounced than in semiconductors. The difference between the thermopower of annealed and cold-worked gold samples (except for low temperatures) is very small [41]. Mechanical stress can thus not be responsible for the observed reduction of the thermopower in gold point contacts, that occurs in the whole investigated temperature range of 2–300 K.

According to another theory, supported by theoretical and experimental investigations on metallic and semiconducting point contacts, the reduction of the thermopower is due to the *suppression of the phonon drag effect* [4, 5, 10, 14]. The thermopower consists of two contributions: the diffusion part, that is caused by the thermal motion of the electrons from the hot side to the cold side of the sample, and the phonon drag part, that is due to momentum transfer from the phonons to the electrons by scattering. The phonons, participating in scattering, are mainly long wavelength modes with a large mean free path. If the contact size is decreased below the mean free path, the propagation of the phonons is affected by boundary scattering, so that the phonon drag part of the thermopower is reduced or even fully suppressed.

In gold the phonon drag effect reaches its maximum value (depending on the purity of the sample material) at a temperature of about 30 K. At higher temperatures, the phonon drag effect becomes less important due to the increasing frequency of phonon–phonon collisions. At room temperature the phonon drag part of the thermopower is negligibly small compared to the diffusion part [25, 30].

Our measurements on gold point contacts clearly show that the reduction of the thermopower also occurs at high temperatures, where no phonon drag effect is present. This is demonstrated by the curves shown in Fig. 7, where the thermopower is plotted as a function of the contact resistance. The suppression of the phonon drag effect can thus not be the reason for the observed reduction of the thermopower.

As has already been mentioned, mechanical point contacts are mostly covered by *surface layers which form a tunneling barrier* with high electrical resistance. In case of electronic heat transport, the

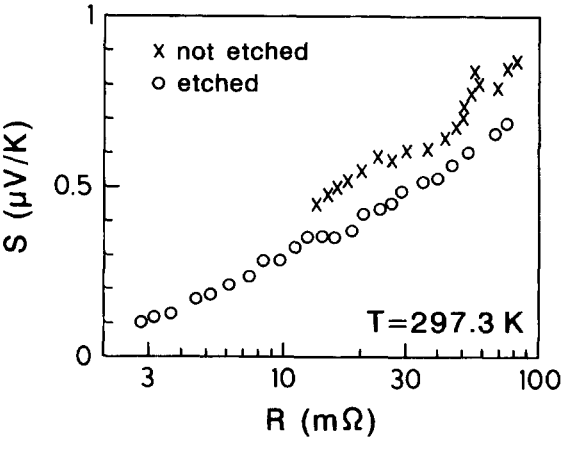

Fig. 7. Measured thermopower $S = S_b - S_{pc}$ as a function of the contact resistance R before and after etching of the samples (S_b and S_{pc} denote the thermopower of the bulk material and the point contact, respectively). The measurements are carried out at a temperature of $T = 297$ K.

electrical resistance is accompanied by a thermal resistance that creates a temperature drop across the tunneling barrier. According to theoretical calculations the temperature drop across the barrier considerably decreases the thermopower of the point contact [31]. The theory is confirmed by measurements on gold and platinum contacts, which show that the observed dependence of the thermopower on the contact size can be explained by tunneling [7–9]. The authors observed that the measured thermopower partly or even completely disappeared when the measurements are carried out at freshly cleaned samples (the cleaning was performed by mechanically removing the surface layer). Even very thin films with a thickness of one atomic layer were found to be sufficient to modify the thermopower.

Our measurements on gold point contacts show rather similar results. In Fig. 7 the thermopower is plotted as a function of the electrical contact resistance before and after etching of the sample surface. The measuring signal is noticeably reduced by etching. This result provides further evidence that the observed behavior of the thermopower is mainly caused by the existence of surface layers.

Another measurement that shows the temperature dependence of the thermopower $S = S_b - S_{pc}$ at *fixed contact size* is presented in Fig. 8. The measuring curve closely follows the form of the bulk thermopower as is known from the literature [30]. This indicates that the thermopower of the investigated point contact S_{pc} is much smaller than the bulk value S_b. Since the described effect occurs in the whole covered temperature range from about 2 to 60 K, we believe that the thermoelectrical properties of the contact are essentially determined by tunneling.

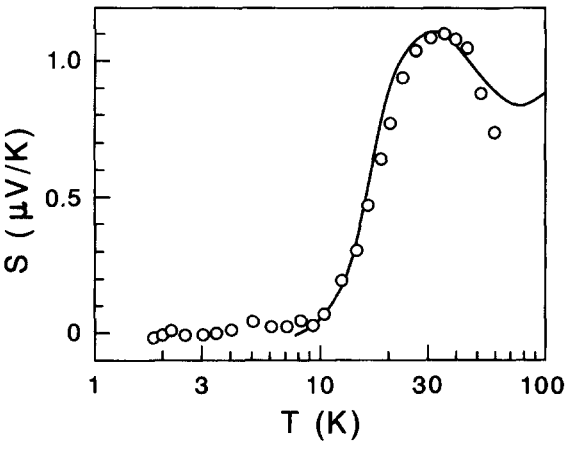

Fig. 8. Temperature dependence of the measured thermopower $S = S_b - S_{pc}$ at fixed contact size. The solid line represents the bulk thermopower S_b according to Ref. [30]. The measurements shown in Figs. 4 and 8 are performed at the same point contact with a resistance of $R \simeq 0.3\,\Omega$.

4.4. Heat asymmetry

Investigations of the heat asymmetry have been performed so far on point contacts consisting of copper, silicon and gallium arsenide. In the experiments on copper contacts, which were carried out at a temperature of $T \simeq 0.7$ K, a heat asymmetry of $\alpha \simeq 0.15$ was found [17]. Unfortunately, we do not know the experimental details, so that the reliability of the measuring results cannot be judged. Measurements on silicon and gallium arsenide were performed by members of our own group some years ago and revealed a heat asymmetry of up to $\alpha = 0.3$ at room temperature [12, 18, 19]. We have repeated these measurements, in the meantime, with an improved measuring device at low temperatures and find an absence of the heat asymmetry within an experimental accuracy of about 1%. A careful re-examination of the earlier applied measuring method taking into account the more detailed insight into point contact transport phenomena gained in the last decade, lead us to the conclusion that the heat asymmetry, that was observed in the older measurements, was pretended by the release of Peltier heat at the electrical contacts. Now we are able to verify this effect by carrying out the same experiments at low temperatures, where the Peltier effect is very small. At low temperatures the apparent heat asymmetry thus disappears.

In the present work we firstly investigate the heat asymmetry of gold point contacts. The measurements are carried out with several contacts of different size in the temperature range 2–300 K. The experiments are partly performed in ultra-high vacuum in order to avoid surface contamination. The samples are cleaned by argon sputtering and

checked by Auger spectroscopy. The heating current is adjusted to $I \simeq 5$–40 mA, corresponding to voltages of $V \simeq 5$–20 mV at the point contact. The accuracy of the measuring results is estimated to be better than 0.5%.

The result of these measurements is always the same, namely a total absence of the heat asymmetry. We thus believe that ballistic charge transport (the condition of asymmetric heat generation) is prevented by a tunneling barrier at the contact surface. Considering the results of the preceding sections of this paper, the tunneling barrier is probably due to surface layers which arise from the adsorption of gas molecules. (Since all measured data yield the same value, $\alpha = 0$, we refrain from drawing a graph of the heat asymmetry.)

5. Summary

In the present work we perform measurements of the electrical resistance, the thermal resistance and the thermoelectric power of gold point contacts. We also investigate carefully the heat asymmetry in the contact area and measure the second derivative of the current–voltage characteristic.

The used measuring device provides optimized conditions for the detection of thermal and thermoelectric phenomena. It enables precise determination of the heat flow across the point contact and prevents perturbing effects such as the generation of Peltier heat at the connecting leads. The available temperature range reaches from 2 to 300 K. To avoid surface contaminations the experiments are partly performed in ultra-high vacuum.

Our measurements clearly indicate that the electrical and thermal resistance of gold point contacts considerably differ from the Wiedemann–Franz-law. The deviations, which are due to the existence of surface layers, can be reduced by etching or sputtering of the sample surface. However, even with cleaned contacts the electrical resistance is temperature independent, which indicates that charge transport mainly takes place by tunneling.

Reduction of the contact size strongly decreases the thermoelectric power of gold point contacts. This effect occurs at high as well as at low temperatures according to our experiments. The reduction of the thermopower can thus not be due to the suppression of the phonon drag effect as supposed in previous investigations.

From our measurements of Joule's heat release in gold point contacts it seems that the heat is generated symmetrically with respect to the contact plane. The absence of asymmetric heat release, despite suitable geometrical conditions, indicates that ballistic charge transport is prevented by surface effects.

Considering all measured data, we conclude that the transport properties of gold point contacts strongly depend on the detailed physical and chemical consistence of the sample surface. Even very thin films with a thickness of only one atomic layer obviously are sufficient to prevent ballistic charge transport by the occurrence of tunneling phenomena. In agreement with this observation most of the investigated phenomena can be attributed to the existence of a tunneling barrier at the contact surface. The influence of the contact size on the transport properties of gold point contacts seems to be comparatively small.

Acknowledgements

We gratefully acknowledge the help of K. Ripka in sample preparation. The experimental equipment was partly financed by the Stiftung Volkswagenwerk, Hannover.

References

[1] A.M. Duif, A.G.M. Jansen and P. Wyder, J. Phys.: Condens. Matter 1 (1989) 3157.
[2] A.D. Wieck and K. Ploog, Appl. Phys. Lett. 56 (1990) 928.
[3] E.N. Bogachek and A.G. Shkorbatov, Fiz. Nizk. Temp. 11 (1985) 643 [Sov. J. Low Temp. Phys. 11 (1985) 353].
[4] E.N. Bogachek, I.O. Kulik and A.G. Shkorbatov, Fiz. Nizk. Temp. 11 (1985) 1189 [Sov. J. Low Temp. Phys. 11 (1985) 656].
[5] E.N. Bogachek, I.O. Kulik, A.N. Omel'yanchuk and A.G. Shkorbatov, Pis'ma Zh. Eksp. Teor. Fiz. 12 (1985) 519 [JETP Lett. 41 (1985) 633].
[6] A.G. Shkorbatov and T.Z. Sarkisyants, Fiz. Nizk. Temp. 19 (1993) 1240 [Low Temp. Phys. 19 (1993) 881].
[7] I. Dietrich, Z. Angew. Phys. 1 (1949) 377.
[8] I. Dietrich and E. Rüchardt, Z. Naturforschg. 4a (1949) 482.

[9] I. Dietrich, Z. Angew. Phys. 2 (1950) 128.
[10] O.I. Shklyarevskii, A.G.M. Jansen, J.G.H. Hermsen and P. Wyder, Phys. Rev. Lett. 57 (1986) 1374.
[11] O.I. Shklyarevskii, A.G.M. Jansen and P. Wyder, Fiz. Nizk. Temp. 12 (1986) 947 [Sov. J. Low Temp. Phys. 12 (1986) 536].
[12] R. Trzcinski, E. Gmelin and H.J. Queisser, Phys. Rev. Lett. 56 (1986) 1086.
[13] L. Weber, E. Gmelin and H.J. Queisser, Phys. Rev. B 40 (1989) 1244.
[14] L. Weber, M. Lehr and E. Gmelin, Phys. Rev. B 46 (1992) 9511.
[15] E.N. Bogachek, A.G. Shkorbatov and I.O. Kulik, Fiz. Nizk. Temp. 15 (1989) 278 [Sov. J. Low Temp. Phys. 15 (1989) 156].
[16] E.N. Bogachek, I.O. Kulik and A.G. Shkorbatov, J. Phys.: Condens. Matter 3 (1991) 8877.
[17] M. Reiffers, K. Flachbart and S. Janos, Pis'ma Zh. Eksp. Teor. Fiz. 44 (1986) 232 [JETP Lett. 44 (1986) 298].
[18] U. Gerlach-Meyer and H.J. Queisser, Phys. Rev. Lett. 20 (1983) 1904.
[19] U. Gerlach-Meyer, Appl. Phys. A 33 (1984) 161.
[20] R. Trzcinski, E. Gmelin and H.J. Queisser, Phys. Rev. B 35 (1987) 6373.
[21] A.G.M. Jansen, A.P. van Gelder and P. Wyder, J. Phys. C 13 (1980) 6973.
[22] A.H. MacDonald and C.R. Leavens, J. Phys. F 13 (1983) 665.
[23] L. Weber and E. Gmelin, Rev. Sci. Instrum. 63 (1992) 211.
[24] R. Holm, Electric Contacts Handbook (Springer, Berlin, 1958) pp. 27–39.
[25] W.B. Pearson, Sov. Phys.-Sol. State 3 (1961) 1024.
[26] D.K.C. MacDonald, W.B. Pearson and I.M. Templeton, Proc. Roy. Soc. London A 266 (1962) 161.
[27] D. Damon, M.P. Mathur and P.G. Klemens, Phys. Rev. 176 (1968) 876.
[28] Y.S. Touloukian, R.W. Powell, C.Y. Ho and P.G. Klemens, Thermophysical Properties of Matter, Vol. 1: Thermal Conductivity of Metallic Elements and Alloys (IFI/Plenum, New York, 1970) pp. 132–137.
[29] N. Cusack and P. Kendall, Proc. Phys. Soc. 72 (1958) 898.
[30] R.S. Crisp and J. Rungis, Phil. Mag. 22 (1970) 217.
[31] M. Kohler, Ann. Phys. (Leipzig, Folge 5) 38 (1940) 542.
[32] E.L. Wolf, in: Solid State Physics 30, eds. H. Ehrenreich, F. Seitz and W. Turnbull (Academic Press, New York, 1975) pp. 4–11.
[33] I.K. Yanson, Phys. Scripta T 23 (1988) 88.
[34] I.O. Kulik, R.I. Shekhter and A.G. Shkorbatov, Zh. Eksp. Teor. Fiz. 81 (1981) 2126 [Sov. Phys. JETP 54 (1981) 1130].
[35] I.O. Kulik, Phys. Lett. 106 A (1984) 187.
[36] J.W. Lynn, H.G. Smith and R.M. Nicklow, Phys. Rev. B 8 (1973) 3493.
[37] A.G.M. Jansen, F.M. Mueller and P. Wyder, Phys. Rev. B 16 (1977) 1325.
[38] J. Tauc, Czechosl. J. Phys. 6 (1956) 108.
[39] J. Tauc, Photo and Thermoelectric Effects in Semiconductors (Pergamon Press, Oxford, 1962) Chs. 4.6 and 4.7.
[40] Z. Trousil, Czechosl. J. Phys. 6 (1956) 178.
[41] W.B. Pearson, Can. J. Phys. 38 (1960) 1048.